A Master Curve for the Shear Degradation of Lubricating Greases with a Fibrous Structure

Yuxin Zhou, Rob Bosman & Piet M. Lugt

A Master Curve for the Shear Degradation of Lubricating Greases with a Fibrous Structure

Yuxin Zhou[a], Rob Bosman[a], and Piet M. Lugt[a,b]

[a]Laboratory of Surface Technology and Tribology, Faculty of Engineering Technology, University of Twente, Enschede, The Netherlands; Laboratory of Surface Technology and Tribology, University of Twente, Enschede, The Netherlands; [b]SKF Research and Technology Development, Nieuwegein, The Netherlands

ABSTRACT

In this article, the mechanical aging behavior of lubricating greases with a fibrous structure is studied by aging fresh samples at controlled shear rates and temperatures in an in-house-made Couette aging machine. The rheological properties of fresh and aged samples were evaluated in a plate–plate rheometer. In the absence of oxygen, no chemical reactions occurred. The results showed that shear degradation is accelerated by increasing the temperature. This thermal effect can be described by an Arrhenius law. A grease aging master curve was created to describe the influence of shear and temperature on the mechanical aging of fibrous structured grease. Next, the model was validated using a conventional grease worker test. Finally, the model was applied to full ball bearings using an R0F + bearing test rig. The master curve forms an important contribution to the development of grease life models.

Introduction

Grease is widely used as a lubricant in rolling bearings. It is often preferred over oil because it does not easily leak out of the bearing and has good sealing properties (Lugt (1)). After the churning phase, the grease forms reservoirs from which lubricant is released to the contacts to separate the rolling elements from the rings by a lubricant film. At some point in time, the grease is no longer able to lubricate, which is called the end of grease life. Generally, the limited life span of the grease determines the life of the bearing. This can be overcome by relubrication; a reasonable relubrication interval can be calculated using grease life models (Lugt (1)). Generally, grease life is determined by two effects: mechanical deterioration (the dominating mechanism at low and moderate temperature; e.g., below 70°C) and chemical deterioration (mainly at high temperature; e.g., higher than 120°C; Lugt (1); Ito, et al. (2)). The present article addresses the first aspect: mechanical degradation.

Mechanical degradation of a grease is mainly caused by pressure and shear. Grease may soften during aging and possibly leak out of the bearing (Lundberg and Höglund (3)); on the other hand, thickening/stiffening may occur, resulting in a loss of oil bleeding capacity (Lugt (1); Salomonsson, et al. (4); Couronne and Vergne (5)). This grease aging behavior is highly dependent on the operating/working conditions (including temperature), chemical composition of the grease, and the grease thickener microstructure.

Spiegel, et al. (6) assumed a particle thickener microstructure and described the degradation process using a fatigue model. Moore and Cravath (7) aged soap-based greases using the roll stability test to study the breakdown of the thickener structure. They proposed an exponential model indicating that the decreasing rate of the change in grease consistency is proportional to the breakage rate of the thickener structure; that is, the thickener geometry was used as a gauge to monitor the grease aging process. Czarny (8) developed an empirical equation describing the drop of grease viscosity in terms of the number of shear cycles applied. Using Czarny's equation, Plint and Alliston-Greiner (9) proposed a half-life parameter to describe the grease aging inside a grease worker: the half-life was defined as the time at which the grease has lost half of its initial viscosity. However, these empirical models are often limited to the specific aging test rigs, and a universal aging model that is capable of describing the grease aging in various conditions still remains unavailable.

To give a common description of degradation dynamics, Bryant, et al. (10) employed entropy as a fundamental measure of degradation and applied this thermodynamic concept to characterize the degradation process of adhesive and fretting wear. Rezasoltani and Khonsari (11) applied this theory on the mechanical aging of grease. By shearing lithium complex greases in a rheometer at relatively low temperatures (25–45 °C), a linear relationship between the generated entropy and the grease aging behavior (change of

Nomenclature

C_e	Correcting factor for the bearing aging energy		R_a	Surface roughness of the measuring plates (centerline average, μm)
C_T	Arrhenius correction factor			
E_b	Bearing friction energy density (J/mm^3)		S_g	Generated entropy per unit volume during aging (J/mm^{3}K)
E_{gw}	Input work density inside the grease worker (J/mm^3)			
E_m	Corrected energy density during the Couette aging procedure (J/mm^3)		T	Applied temperature during aging (°C)
			T_0	Reference temperature (°C)
F_a	Axial load applied in the R0F + test (N)		t	Grease aging time (s)
F_{gw}	Drag force generated inside the grease worker (N)		t_b	R0F + bearing running time (s)
F_r	Radial load applied in the R0F + test (N)		V_a	Grease volume inside the Couette aging machine (mm^3)
K	Coefficient of degradation			
L_{50}	Estimated bearing life at which 50% of the bearing population has failed (h)		V_b	Grease filling volume inside the R0F + test bearings (mm^3)
L_{piston}	Length of a stroke in the grease worker (m)		V_{gw}	Grease volume inside the grease worker (mm^3)
M	Torque (Nm)		W	Input work during the Couette aging procedure (J)
M_{rr}	Rolling frictional moment generated from the R0F + bearing (Nm)		Y	Rheological properties of the grease during aging
			Y_∞	Second-stage rheological value after infinitely long aging
M_{sl}	Sliding frictional moment generated from the R0F + bearing (Nm)		Y_i	Initial rheological value for fresh grease
			$\dot{\gamma}_a$	Aging shear rate (s^{-1})
N	Rotational speed (rpm)		$\dot{\gamma}_{ps}$	Shear rate for preshear (s^{-1})
n	Degradation exponent		τ_y	Yield stress obtained from the oscillatory strain sweep test (Pa)
R^2	Goodness value of the fitting			

consistency) was found. They later used this concept to build a shear life model (Rezasoltani and Khonsari (12)), in which the grease life was determined by the time at which a critical consistency would be reached. In an earlier paper (Zhou, et al. (13)), the current authors also used this entropy concept to develop a master curve for the shear degradation of grease. However, when performing prolonged aging tests in a Couette aging machine, the results showed that this linear aging behavior was not able to fully describe the grease shear aging process: the grease aging rate was found to decrease in time, ultimately showing asymptotic behavior where the aging process practically ends. This is plausible; after all, because the size of the thickener fibers decreases in time, there is a reduced probability for breakage of these fragmented fibers, resulting in a continuous reduction in the aging rate (Moore and Cravath (7)). Similar grease aging behavior was shown in the literature (Lugt (1); Spiegel, et al. (6)). Therefore, an exponential aging equation was proposed (Zhou, et al. (13)).
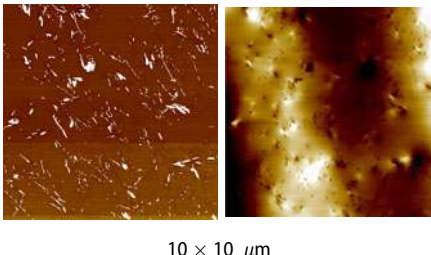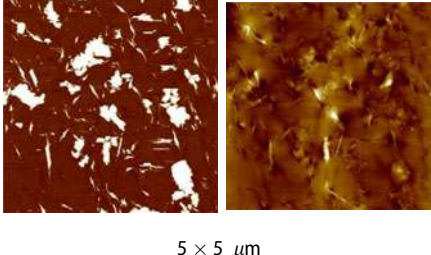
The mechanical aging tests described above were performed at relatively low temperatures; that is, at the low ends of the "green temperature window" (Lugt (1)), where chemical degradation is not dominant. In addition to oxidation, grease will experience thermal degradation (Hurley, et al. (14)). Couronne and Vergne (5) worked on the thermal aging of lithium-thickened greases. Their rheological evaluation and microstructure measurements showed that at elevated temperature (150°C), lithium grease was weakened, even in the absence of oxidation. Plint and Alliston-Greiner (9) sheared lithium grease in a self-made viscometer. They observed that when aging at high temperatures, the influence of shearing on the grease's viscosity loss is more pronounced. Cyriac, et al. (15) studied the temperature dependency of the yield stress for various greases and found that for both lithium- and polyurea-thickened greases, the

yield stress reduces by a factor of 2 by a certain temperature increase. A decrease in grease yield stress at higher temperature was also shown by Karis, et al. (16), Gow (17), and Froishterer (18). Ide, et al. (19) predicted the grease life of lithium soap–thickened grease using thermogravimetry tests. They concluded that the activation energy based on Arrhenius's law is an appropriate parameter in grease life prediction. To summarize: to capture the mechanical aging of grease, the mechanical work put into the grease (shear) as well as temperature play a role. A grease aging master curve should therefore take both factors into account.

The current article extends the work that was earlier published in Zhou, et al. (13) where the shear degradation was described at a fixed temperature. The influence of temperature on shear degradation will be included in this study. The results show that elevated temperatures accelerate aging due to the possible change in thickener properties (Salomonsson, et al. (4); Couronne, and Vergne (5); Bondi, et al. (20)), which is not well described by the entropy concept (Rezasoltani and Khonsari (12); Zhou, et al. (13)). It will be shown that grease degradation is determined by the energy density where the Arrhenius equation should be used to include thermal effects, called corrected energy density, E_m, here. Oxidation did not occur, which was confirmed by Fourier transform infrared (FTIR) measurements. Based on this, a modified grease aging master curve has been developed and validated using a conventional grease worker test (ASTM D217) equipped with a load sensor to measure the work exerted on the grease.

At the end of this article, the master curve will be applied to the aging in full bearings; that is, grease aged using a R0F + grease tester equipped with deep-groove ball bearings. The results show that although grease aging is more complex inside rolling bearings, the overall aging behavior demonstrates a trend similar to that described by the proposed curve. Based on this, a potential application of the master

Table 1. Composition and properties of the tested greases.

Grease	Thickener	Mass fraction of the thickener	Base oil	Base oil viscosity at 40°C/100°C	NLGI	AFM phase contrast	AFM topography image
LiX/PAO	Lithium complex	0.20	PAO	191/42 cSt	2–3		
							10×10 μm
PU/E	Polyurea	0.26	Synthetic ester	70/9.4 cSt	2–3		
							5×5 μm
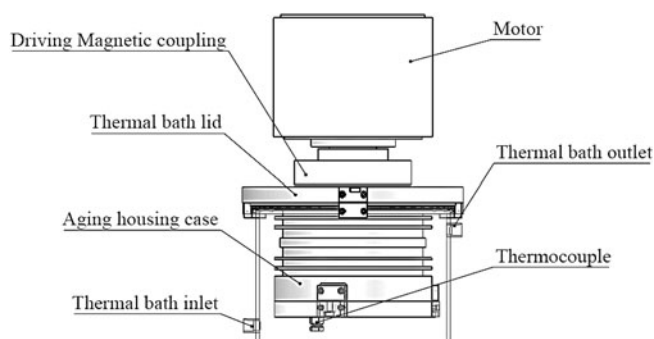
Figure 1. Schematic drawing of the Couette aging machine.

curve on grease life prediction inside a deep-groove ball bearing will be illustrated.

Materials and methods

Tested grease

Commercial greases based on two types of thickeners combined with different base oils were tested; that is, a lithium complex soap grease with poly-alpha-olefin (PAO) base oil, denoted by LiX/PAO, and polyurea-thickened grease with ester base oil, denoted by PU/E. Both greases have a fiber-like thickener structure. Some relevant information about these greases is summarized in Table 1. The microstructure of the grease thickener was obtained using atomic force microscopy (AFM) in tapping mode.

Shear aging test

During practical usage, grease will experience both shear and thermal stress. To perform grease aging at both controlled shear rates and temperatures, a new aging machine was designed and built. The machine is here referred to as the Couette aging machine.

Figures 1 and 2 show a schematic overview of the aging setup. To ensure homogeneous shear, the grease will be
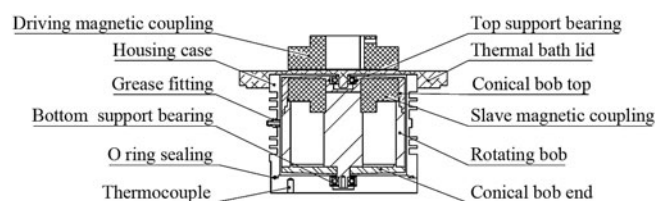
Figure 2. Schematic drawing of the aging head.

sheared between a cylindrical housing and a biconical bob. The angle of the conical ends was chosen such that a similar shear rate field will occur in the conical and cylindrical sections of the working head (Malkin, et al. (21)). One of the challenges is keeping the grease in the Couette geometry because, due to the Weissenberg effect, the grease will flow upwards in the gap. This was accomplished by driving the rotating bob via a magnetic coupling through a stainless steel lid. Additionally, grease leakage, evaporation of base oil, and oxidation of the grease are limited due to the airtight seal created by the lid and an o-ring. To ensure a proper alignment of the bob, two small ball bearings are placed inside the aging head. Before an aging test, fresh grease is injected via the grease fitting (Fig. 2). Once completely full, the aging head is closed and immersed in the thermal bath.

During aging, the temperature is recorded from the thermocouple at the bottom of the housing case; see Figs. 1 and 2. From the motor current, the torque and therefore the generated drag when shearing the grease can be calculated by subtracting the reference torque value, which was recorded when running the Couette aging machine with no grease filling inside the aging head.

To study the influence of temperature on aging, grease will be aged at controlled temperatures for specific aging periods. The aging temperatures were chosen as 50, 85, and 120 °C. The highest aging temperature was selected as 120°C, which is considered the highest acceptable working temperature for standard lithium soap–thickened grease in ball bearings (Couronne and Vergne (5)). The shear rate was selected equal to one of the values applied in the

Table 2. Shear aging condition.

Aging at constant shear rate $\dot{\gamma}_a = 175\ s^{-1}$	PU/E	50°C	5 h, 25 h
		85°C	5 h, 8 h, 40 h
		120°C	5 h, 10 h, 50 h
	LiX/PAO	50°C	5 h, 10 h, 25 h, 50 h
		85°C	10 h, 19 h, 50 h
		120°C	10 h, 17 h, 29 h
Mixed aging (PU/E)			Aged at 85°C, 350 s^{-1} for 1 h, followed by aging at 50°C, 175 s^{-1} for 1 h
			Aged at 50°C, 175 s^{-1} for 2 h, followed by aging at 25°C, 350 s^{-1} for 2 h

Table 3. Thermal aging conditions.

	Heating time (h)	
Temperature (°C)	LiX/PAO	PU/E
50	2, 5, 8, 20, 100	2, 5, 10, 20, 40, 120
85	2, 5, 8, 20, 100	2, 5, 10, 20, 40, 120
120	2, 5, 8, 20, 100	2, 5, 10, 20, 40, 120

previous paper: $\dot{\gamma}_a = 175\ s^{-1}$ (Zhou, et al. (13)). The input work W was calculated as

$$W = \int \frac{M \cdot N \cdot 2\pi}{60}\ dt, \qquad [1]$$

where the torque M (N · m) and rotational speed N (rpm) were collected from the motor; t is the aging time in seconds.

To verify that the aging process is independent of the applied shear rate (presented in the earlier work; Zhou, et al. (13)), aging tests were performed on fresh PU/E using various shear rates. The aging conditions in the Couette aging machine are listed in Table 2.

Thermal aging test

Thermal aging tests were performed by inserting 11 g of fresh grease into a glass bottle, sealed by aluminum foil. The sealed samples were subsequently heated in an oven at various temperatures. This makes it possible to investigate the influence of only temperature on the grease aging properties. Temperatures and time spans similar to those used for the Couette aging machine tests were selected. The test conditions are shown in Table 3.

ROF + test

To study the grease aging inside a bearing, fresh PU/E was aged using an SKF ROF + test rig. The ROF + is a test rig designed to determine grease life, where two pairs of deep-groove ball bearings (two test bearings and two support bearings) are tested under specific temperature, speed, and load for prolonged running (Lugt (1); Lugt, et al. (22)). In these grease aging tests, the bearings were shielded and filled with approximately 30% of the bearing free volume using fresh PU/E (giving an initial fill volume of $V_b = 1.6 \times 10^3$ mm^3). To avoid bearing failures (because the goal is to study grease degradation), the applied load should be relatively low but high enough to prevent skidding.

Two test conditions were selected, under which the bearings were run for specific periods of time but always shorter than the estimated grease life. The ROF + test conditions are

shown in Table 4. Then the worked PU/E was collected from the bearing and mixed to form a homogenous structure, because the volumes were too small to collect grease from specific locations inside the bearing. Most of the grease was collected on the inner surface of the shield as shown in Fig. 3.

Sample characterization

To evaluate the change in grease properties from the aging tests, the yield stress was measured for fresh and aged grease samples in an MCR 501 Anton-Paar rheometer using a plate–plate geometry, with 1-mm measuring gap (sufficiently high compared to the tested grease fiber length) and roughened surfaces (top plate: $R_a = 1.5$ μm; bottom plate: $R_a = 2.3$ μm) to decrease wall-slip effects. Once the sample was loaded, preshear was applied following the DIN standard (Deutsches Institut für Normung (23); $\dot{\gamma}_{ps} = 100$ s^{-1} for 60 s at 25°C). After 30-min relaxation time, oscillatory strain sweep measurements were performed, where the shear strain ranged from 10^{-3}% to 10^3% at 1 Hz and 25°C. Based on the stress–strain curve, the yield stress τ_y was obtained at the point where a predefined deviation from the linear stress–strain behavior takes place (Cyriac, et al. (24)). For every tested sample, at least two rheological measurements were performed. In the rest of this article, the aging results will be plotted as a marker indicating the average value with the corresponding measuring spread. In addition, to check whether chemical reactions took place during aging, FTIR measurements were carried out for both fresh and aged samples.

Results and discussion

Entropy concept trial

In our previous paper (Zhou, et al. (13)), the entropy concept was applied to describe the aging process of lithium soap grease (with a fibrous thickener structure) at multiple shear rates. There were no data to show that the concept would properly include the effect of temperature. Therefore, additional tests on the Couette aging machine for different temperatures have now been conducted. The entropy density S_g is calculated by dividing the input work W over the grease sample volume V_a and the aging temperature T (Rezasoltani and Khonsari (11)):

$$S_g = \frac{W/V_a}{T}. \qquad [2]$$

The yield stress variation during aging for both LiX/PAO and PU/E is plotted against the entropy generation density in Fig. 4. This figure shows different aging curves for different temperatures, which implies that the entropy generation density is not the suitable parameter to describe aging.

Table 4. ROF + test condition.

	Running temperature (°C)	Axial load F_a (N)	Radial load F_r (N)	Rotational speed N (rpm)	Running time (h)
Condition 1	120	500	50	10,000	22, 195
Condition 2	120	270	70	15,000	100, 235, 600

Figure 3. Sample collection after ROF + test.

In order to include thermal effects in the shear aging model, first pure thermal aging will be addressed in the absence of shear.

Thermal aging results

To study only the effect of the elevated temperature on grease aging, time sweep isothermal aging tests were performed on fresh LiX/PAO and PU/E at 50, 85, and 120 °C. According to the FTIR spectra, no extra peak is observed, confirming the absence of oxidation; see Fig. 5.

The thermal aging results are shown in Fig. 6, where the yield stress versus the logarithmic heating time at different temperatures was plotted. Clearly, for each temperature, the yield stress shows a descending trend versus the heating time. In addition, when baked at higher temperature, the aging rate increases, which agrees with the Couette aging machine test observation as shown in Fig. 4.

Couronne and Vergne (5) attributed this thermal effect on grease aging to the variation in thickener structure. They concluded that high temperature makes the fibers more brittle and therefore breakage of such fibers will be easier. Salomonsson, et al. (4) made similar observations: after 7 days' aging inside a beaker at 120°C, the thickener fiber length decreased from 1 to 0.1 μm, whereas the average fiber diameter increased from 30 to 50 nm. Huang, et al. (25) attributed the fiber shortening of lithium soap–based grease to the loss of physical bonding of thickener molecules at high temperature (120 °C). These observations may very well explain why grease deteriorates faster at higher temperature: thermal weakening.

The three isothermal aging curves in Fig. 6 could be merged together by correcting the thermal aging time t (h) with an Arrhenius correction factor C_T at a reference temperature T_0: for LiX/PAO $C_T = 2^{\frac{T-T_0}{15}}$ and for PU/E $C_T = 2^{\frac{T-T_0}{10}}$. In the current study, room temperature (25°C) is selected as the reference value, so $T_0 = 25$°C. In this way, the isothermal heating time is transferred to the heating time at reference temperature and a temperature-independent curve is fit; see Fig. 7.

The fitting results shown in Fig. 7 suggest that for LiX/PAO, the thermal effect on the change of yield stress can be expressed as

$$\tau_y = -2.3 \ ln(t \cdot C_T) + 56, \qquad [3]$$

and for PU/E as

$$\tau_y = -4.5 \ ln(t \cdot C_T) + 90. \qquad [4]$$

This reduction in yield stress with increasing temperature is likely to be one of the reasons for the reduction in grease life with increasing temperature. It is apparent that the factor of 10 and 15°C for a reduction in yield stress with a factor of 2 is similar to the reduction in grease life with a factor of 2 (Lugt (1); Kawamura, et al. (26)).

A master curve for grease aging

It was shown above that in the absence of oxygen, grease thermal aging can be described as a function of temperature by correcting the isothermal heating time using the Arrhenius correction factor C_T. When evaluating the grease aging inside the Couette aging machine, the input work was calculated by integrating the product of torque and speed over the aging time (Eq. [1]). Because both thermal aging behavior in the oven and shear aging behavior in the Couette aging machine are described as a function of time, the applied work is used with an Arrhenius temperature correction (here called corrected energy density, E_m), giving a master curve for the mechanical aging of grease, taking both temperature and shear effects into account. The corrected energy density E_m then reads

$$E_m = \frac{C_T \cdot W}{V_a}, \qquad [5]$$

where W is the mechanical work; C_T is the Arrhenius correction factor, which was derived from the pure thermal aging tests; and V_a is the grease volume inside the Couette aging machine. Here the reference temperature is again $T_0 = 25$°C. Note that the unit for E_m is J/mm3.

The aging results for PU/E and LiX/PAO in terms of E_m are presented in Figs. 8 and 9. As shown in the figures, when plotted against the corrected energy density E_m, the aging behavior shows a trend similar to that for the shear degradation of lithium grease in the previous study (Zhou, et al. (13)): a progressive degradation phase at the beginning and slower degradation afterwards. Therefore, the previous developed grease aging model is applicable in an adapted form, where the generated entropy density S_g is replaced by the corrected energy density E_m:

$$Y = \frac{Y_i - Y_\infty}{1 + K \cdot E_m{}^n} + Y_\infty, \qquad [6]$$

where Y represents the rheological property (in this case the yield stress), with the index i representing the initial
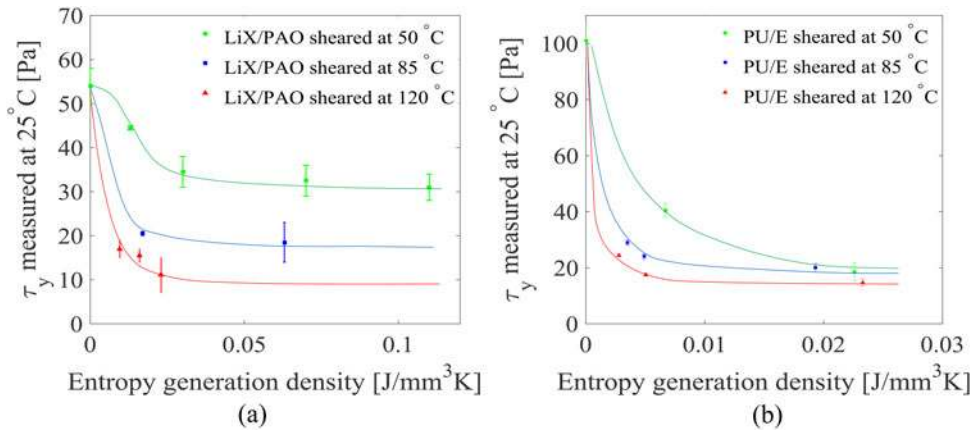
Figure 4. Yield stress vs. entropy generation density at various aging temperatures for (a) LiX/PAO and (b) PU/E.
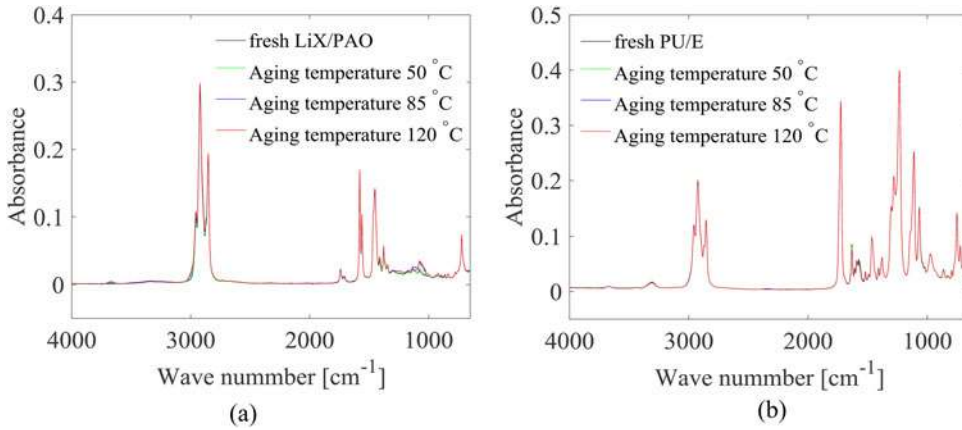

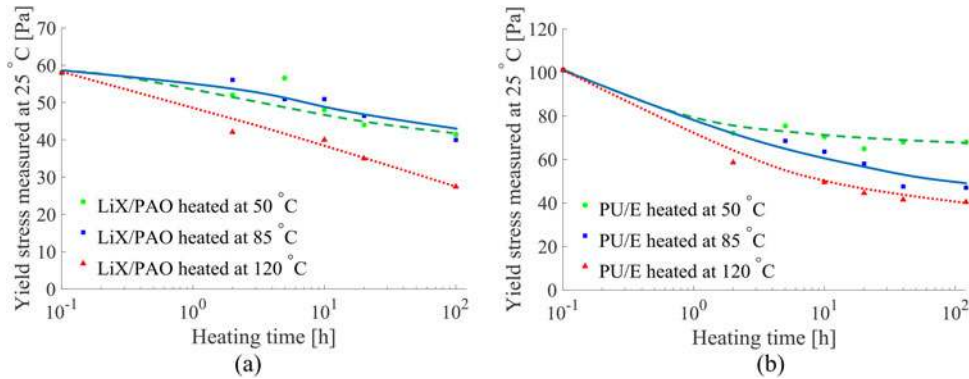**Figure 5.** FTIR comparison between the fresh and thermal aged (a) LiX/PAO and (b) PU/E.

Figure 6. Yield stress (measured at 25°C, 1 Hz) for purely thermal aged samples: (a) LiX/PAO and (b) PU/E.

rheological value for fresh grease and ∞ representing the second-stage value for the sample aged for a long time; K and n are the coefficient of degradation and the exponent of degradation obtained from the curve fitting. This aging model fits well for both PU/E and LiX/PAO; see Figs. 8 and 9 as well as Table 5. Clearly, when applying the corrected energy density E_m, the grease aging behavior inside the Couette aging machine can now be described independent of the aging shear rate and aging temperature.

A grease with a higher degradation coefficient K and exponent n is more fragile and sensible to shear. Reaching the second phase of grease degradation inside a bearing does not mean that the fragmented thickener, together with the base oil,

will no longer function as a lubricant. On the contrary, it was shown previously that grease with smaller thickener particles generates thicker films than grease with larger thickener particles (Cyriac, et al. (27)). However, the destruction of the thickener network will have an effect on grease bleed and grease consistency, which again will have an impact on the grease performance and may determine the grease life inside a bearing.

Validation of the master curve aging model

Thus far, the grease aging model has been developed based on samples prepared in the in-house-made Couette aging machine, where grease is subjected to uniform shear only.
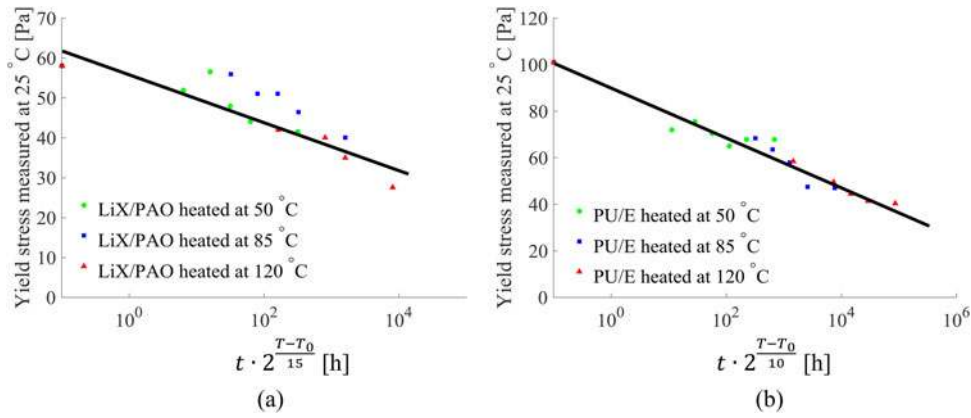
Figure 7. Pure thermal aging results using the Arrhenius correction factor: (a) LiX/PAO and (b) PU/E.
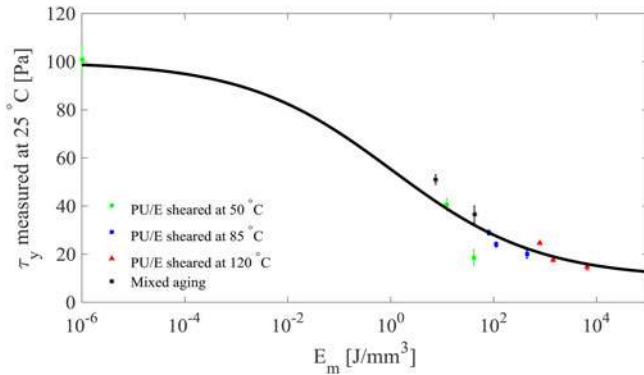

Figure 8. Yield stress vs. E_m for PU/E aged inside the Couette aging machine.

Table 5. Parameters for the master curve equation.

	Y_i (τ_y Pa)	Y_∞ (τ_y Pa)	K	n	Goodness-of-fit value R^2
LiX/PAO	54	10	0.04	0.89	0.94
PU/E	100	10	1.1	0.34	0.97

Table 6. Aging strokes for PU/E inside the DIN grease worker.

Number of strokes	130	655	6,550	13,100	131,000
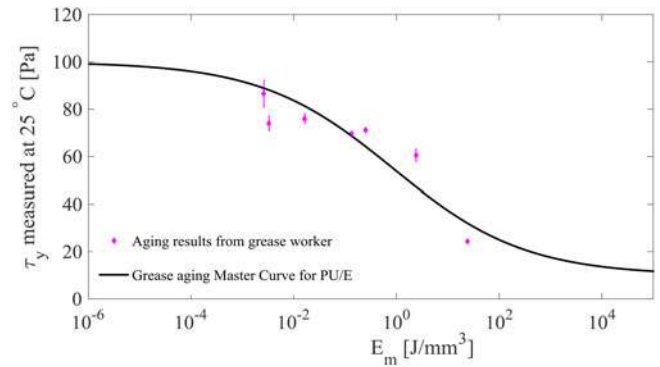
Figure 10. Validation of grease aging master curve for PU/E inside a grease worker.

$$E_{gw} = \frac{\sum F_{gw} \cdot L_{\text{piston}}}{V_{gw}}. \qquad [7]$$

The yield stress of fresh and aged PU/E was plotted against the input energy and the result fits well with the grease aging master curve; see Fig. 10. This suggests that the master curve is generally applicable for prediction/describing the mechanical aging of grease.

Application of the aging master curve to a bearing

In this section, the master curve will be applied to grease aging inside a rolling bearing. The grease flow inside a rolling bearing consists of two phases. After filling the bearing with grease and starting up, the grease will first experience a churning phase, where a large fraction of the grease will be churned and moved toward the unswept area. During this phase, excessive shear on the grease takes place. At the end of this phase, most of the grease has ended up under the cage, on the shield/seal
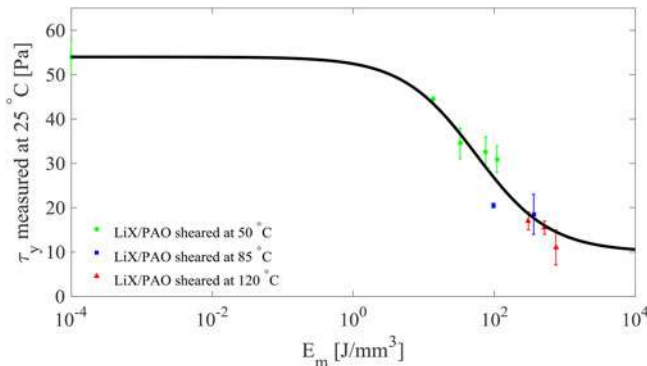

Figure 9. Yield stress vs. E_m for LiX/PAO aged inside the Couette aging machine.

To check whether this concept can be more widely applied, the master curve was also applied to a conventional scaled grease worker where fresh grease was aged at the reference temperature of 25°C varying the number of strokes as listed in Table 6 (DIN ISO D217). This validation test was only carried out using PU/E.

To measure the input energy for the grease worker, the generated drag load F_{gw} during the aging process was recorded by a load cell mounted under the grease worker container. The input energy density E_{gw} was calculated by summing the product of the load F_{gw} and the length of a stroke L_{piston} during the aging process, divided by the grease volume inside the container V_{gw}:

Table 7. ROF + test results for PU/E.

Sample		Bearing frictional torque M (N · m)	Correcting factor C_e	Bearing friction energy density E_b (Jmm^{-3})	Yield stress measured at 25°C (Pa)
Fresh PU/E		0	0	0	100
Condition 1	22 h	3.4×10^{-2}	2.0×10^{-4}	1.7×10^3	63
	195 h			1.5×10^4	58
Condition 2	100 h	2.6×10^{-2}	2.0×10^{-4}	9.0×10^3	43
	235 h			2.1×10^4	52
	600 h			5.4×10^4	30
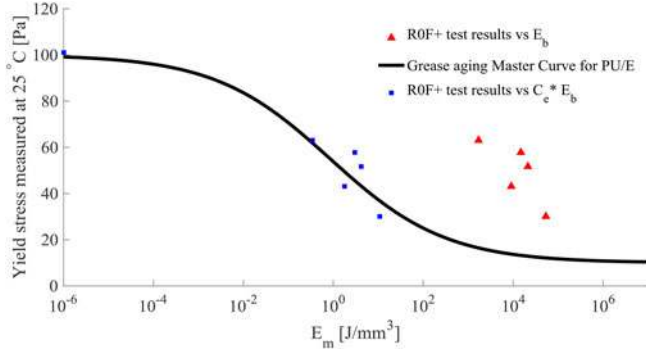
Figure 11. PU/E ROF + results and the Couette aging curve fit.

Figure 12. PU/E grease aging curve based on the ROF + results.

inner surface and bearing shoulders. During the next phase, a fraction of the grease from the reservoirs may fall back into the contact area by, for example, vibrations, cage scraping, or shear caused by (gently) touching the rolling elements (Cann and Lubrecht (28); Lugt, et al. (29)). In this phase, only a fraction of the grease will be sheared. Hence, the grease will not be uniformly aged inside a rolling bearing and calculation of the imposed mechanical work on the grease in a rolling bearing will not be straightforward.

The aging test in a rolling bearing was performed via the ROF + test, using PU/E grease in a deep-groove ball bearings (6204-2Z) for different periods of running time under two test conditions (Table 4). The yield stress for the grease after the bearing test is shown in Table 7. The yield stress decreases as a function of time, similar to aging the grease in the Couette aging machine or grease worker.

The friction energy density inside the bearing E_b was calculated by integrating the product of frictional torque M and angular speed over time (Eq. [1]) divided by the total initial grease filling volume V_b. For the ROF + shielded bearing, the frictional torque M is obtained by making use of the SKF model (SKF Group (30)):

$$M = M_{rr} + M_{sl}, \quad [8]$$

where M_{rr} is the rolling frictional moment and M_{sl} is the sliding frictional moment.

The SKF friction torque model was developed for steady-state running condition; that is, after the churning phase, where the friction torque is more or less stable. Each of the ROF + tests was started with a freshly greased bearing. Therefore, the tests include primarily the starting fraction of a bearing service life and the friction torque M was considered constant during the running time. The calculated frictional torque M and the bearing friction energy density E_b for the ROF + tests are given in Table 7.
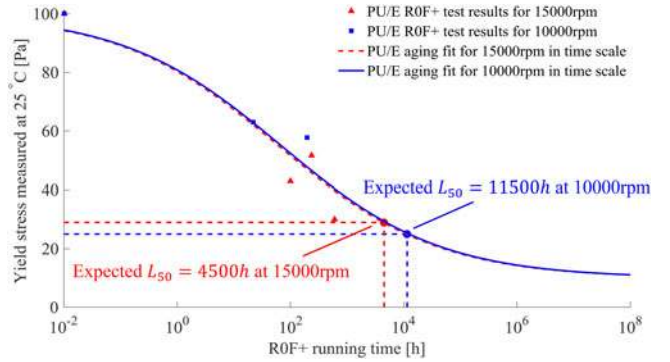
The results are plotted as the yield stress measured at 25°C versus the friction energy density E_b in Fig. 11. The result does not fit onto the master curve. The reasons are obvious: the aged PU/E was collected from the 6204-2Z as a mixture of grease from the various parts of the bearing; that is, from the areas where grease was subjected to shear but also from the areas where the grease was stationary. Therefore, a fraction of the grease will be aged and this volume will be smaller than the total initial fill, which is clearly different from the aging inside the Couette aging machine.

A good fit was obtained by multiplying the frictional energy density with a correcting factor $C_e = 2.0 \times 10^{-4}$ so that the bearing frictional energy density E_b can be translated to the corrected input energy density E_m inside the Couette aging machine:

$$E_m = C_e \cdot E_b. \quad [9]$$

It is no surprise that the C_e value is small. After all, the bearing friction energy density E_b is calculated based on a combination of sliding and rolling friction moment (Eq. [6]), which is larger than the energy dissipated in only shearing the grease. Additionally, inside the bearing, a major fraction of the grease is quite immobile after the churning phase and it is not the total volume of grease that will be severely sheared. This correcting factor C_e is thus applied to correct the grease aging energy and to compensate for the uncertainty in the stressed grease volume and the shear of grease inside the bearing. It is apparent that with the corrected energy ($C_e \cdot E_b$), the ROF + results follow the master curve (Fig. 11). Therefore, the aging master curve can be translated to the bearing running time t_b by making use of Eqs. [1] and [9]:

$$E_m = C_e \cdot E_b = C_e \cdot \frac{\frac{M \cdot N \cdot 2\pi}{60} \cdot t_b}{V_b}, \quad [10]$$

where the unit of the bearing running time t_b is seconds.

Based on the master curve parameters in Table 5 and Eqs. [6] and [10], the translated grease aging curve for PU/E in terms of the R0F + bearing running time t_b reads

$$\tau_y = \frac{100-10}{1 + 1.1 \cdot \left(C_e \cdot \frac{\frac{M \cdot N \cdot 2\pi}{60} \cdot t_b}{V_b} \right)^{0.34}} + 10. \qquad [11]$$

In Fig. 12, the translated grease aging curve for each test condition is plotted with the corresponding R0F + results versus the bearing running time. The two translated curves are very close to each other. This is logical, because the difference in the current two R0F + running conditions and the corresponding bearing frictional torque M is small (see Tables 4 and 7), resulting in similar translated curves.

The grease life calculated from the SKF grease life model (SKF Group (30)) is also plotted on the grease aging curve in Fig. 12, together with the corresponding yield stress value calculated from Eq. [11]: in the case of 15,000 rpm, the grease life inside a 6204-2Z bearing is expected to be $L_{50} = 4,500$ h, when the yield stress would drop to 29 Pa; in the case of 10,000 rpm, $L_{50} = 11,500$ h, when the yield stress would drop to 25 Pa.

It is tempting to use the master curve, with critical yield stress as a method to predict grease life. According to the master curve, the end of grease life for both operating conditions in the R0F + test is reached at an critical value of the yield stress, which is close to the lower limit and suggests that the end of grease life is given by the point in time where the active fraction of the grease has almost lost its consistency. However, this critical yield stress may not be unique. It may be grease, bearing, and operating condition dependent. The evaluation can only be made if the mechanical work the grease experiences inside the bearing is known in detail. This needs to be further investigated in future research and can only be explored using rolling bearing grease life tests.

Conclusion

In this study, the influence of shear and temperature on the aging of fibrous structured greases has been studied by aging grease inside an in-house-made Couette aging machine under controlled shear rate and temperature. The change in rheological properties is a function of the energy per stressed volume. The results demonstrate that increasing temperature accelerates the mechanical aging process and that this thermal effect can be described using an Arrhenius correction factor. Based on this, a grease aging model is constructed using the imposed energy corrected for temperature, leading to a master curve for the mechanical aging of grease. The master curve was validated using a grease worker. It was subsequently applied to grease aged inside deep-groove ball bearings, showing that the concept also applies to grease aging in a rolling bearing. This master curve could be used as a potential building block or screening method for grease life. It is important to mention that the current model only describes shear degradation. A full grease life model should include not only all aging components but also their impact on lubrication performance and can only be validated using rolling bearing grease life tests.

References

(1) Lugt, P. M. (2013), *Grease Lubrication in Rolling Bearings*, John Wiley & Sons: UK.

(2) Ito, H., Tomaru, M., and Suzuki, T. (1988), "Physical and Chemical Aspects of Grease Deterioration in Sealed Ball Bearings," *Lubrication Engineering*, **44**(10), pp 872–879.

(3) Lundberg, J. and Höglund, E. (2000), "A New Method for Determining the Mechanical Stability of Lubricating Greases," *Tribology International*, **33**(3), pp 217–223.

(4) Salomonsson, L., Stang, G., and Zhmud, B. (2007), "Oil/Thickener Interactions and Rheology of Lubricating Greases," *Tribology Transactions*, **50**(3), pp 302–309.

(5) Couronne, I. and Vergne, P. (2000), "Rheological Behavior of Greases: Part II—Effect of Thermal Aging, Correlation with Physico-Chemical Changes," *Tribology Transactions*, **43**(4), pp 788–794.

(6) Spiegel, K., Fricke, J., and Meis, K. (2000), "Die Fließeigenschaften von Schmierfetten in Abhängigkeit von Beanspruchung, Beanspruchungsdauer und Temperatur," *International Colloquium on Tribology*, 3:21.4-121.4-11, 1992, Esslingen, Germany.

(7) Moore, R. J. and Cravath, A. M. (1951), "Mechanical Breakdown of Soap-Base Greases," *Industrial & Engineering Chemistry*, **43**(12), pp 2892–2897.

(8) Czarny, R. (1989), "Einfluss der Thixotropie auf die Rheologischen Eigenschaften der Schmierfette," *Tribologie und Schmierungstechnik*, **36**(3), pp 134–140.

(9) Plint, M. and Alliston-Greiner, A. (1992), "A New Grease Viscometer: A Study of the Influence of Shear on the Properties of Greases," *NLGI spokesman*, **56**(2), pp 7–15.

(10) Bryant, M. D., Khonsari, M. M., and Ling, F. F. (2008), "On the Thermodynamics of Degradation," *Proceedings of the Royal Society A: Mathematical, Physical and Engineering Sciences, 464*, pp 2001–2014.

(11) Rezasoltani, A. and Khonsari, M. M. (2014), "On the Correlation between Mechanical Degradation of Lubricating Grease and Entropy," *Tribology Letters*, **56**(2), pp 197–204.

(12) Rezasoltani, A. and Khonsari, M. M. (2016), "An Engineering Model to Estimate Consistency Reduction of Lubricating Grease Subjected to Mechanical Degradation under Shear," *Tribology International*, **103**, pp 465–474.

(13) Zhou, Y., Bosman, R., and Lugt, P. M. (2018), "A Model for Shear Degradation of Lithium Soap Grease at Ambient Temperature," *Tribology Transactions*, **61**(1), pp 61–70.

(14) Hurley, S., Cann, P., and Spikes H. (2000), "Lubrication and Reflow Properties of Thermally Aged Greases," *Tribology Transactions*, **43**(2), pp 221–228.

(15) Cyriac, F., Lugt, P. M., and Bosman, R. (2016), "Impact of Water on the Rheology of Lubricating Greases," *Tribology Transactions*, **59**(4), pp 679–689.

(16) Karis, T. E., Kono, R. N., and Jhon, M. S. (2003), "Harmonic Analysis in Grease Rheology," *Journal of Applied Polymer Science*, **90**(2), pp 334–343.

(17) Gow, G. M. (1990), The CEY to Grease Rheology," International Tribology Conference 1990, Brisbane *2–5* December 1990: Putting Tribology to Work; Reliability and Maintainability through Lubrication and Wear Technology, Institution of Engineers: Australia, pp 202.

(18) Froishterer, G. (1989), *Rheological and Thermophysical Properties of Greases*, CRC Press.

(19) Ide, A., Asai, Y., Takayama, A., and Akiyama, M. (2011), "New Life Prediction Method of the Grease by the Activation Energy," *Tribology Online*, **6**(1), pp 45–49.

(20) Bondi, A., Cravath, A. M., Moore, R. J., and Peterson, W. H. (1950), "Basic Factors Determining the Structure and Rheology of Lubricating Grease," *The Institute Spokesman*, **13**(12), pp 12–18.

(21) Malkin, A. I., Malkin, A. Y., and Isayev, A. I. (2017), *Rheology: Concepts, Methods & Applications*, Elsevier.

(22) Lugt, P. M., Kommer, A., Lindgren, H., and Deinhofer, L. (2013), "The ROF Methodology for Grease Life Testing," *NLGI Spokesman*, **77**(1), pp 18–27.

(23) Deutsches Institut für Normung. (2007), *Testing of Lubricants—Determination of Shear Viscosity of Lubricating Greases by Rotational Viscosimeter—Part 1: System of Cone/Plate*, Deutsches Institut fur Normung: Author.

(24) Cyriac, F., Lugt, P. M., and Bosman, R. (2015), "On a New Method to Determine the Yield Stress in Lubricating Grease," *Tribology Transactions*, **58**(6), pp 1021–1030.

(25) Huang, L., Guo, D., Cann, P., Wan, G. T., and Wen, S. (2016), "Thermal Oxidation Mechanism of Polyalphaolefin Greases with Lithium Soap and Diurea Thickeners: Effects of the Thickener," *Tribology Transactions*, **59**(5), pp 801–809.

(26) Kawamura, T., Minami, M., and Hirata, M. (2001), "Grease Life Prediction for Sealed Ball Bearings," *Tribology Transactions*, **44**(2), pp 256–262.

(27) Cyriac, F., Lugt, P. M., Bosman, R., Padberg, C., and Venner, C. (2016), "Effect of Thickener Particle Geometry and Concentration on the Grease EHL Film Thickness at Medium Speeds," *Tribology Letters*, **61**(2), pp 1–13.

(28) Cann, P. and Lubrecht, A. (1999), "An Analysis of the Mechanisms of Grease Lubrication in Rolling Element Bearings," *Lubrication Science*, **11**(3), pp 227–245.

(29) Lugt, P. M., Velickov, S., and Tripp, J. H. (2009), "On the Chaotic Behavior of Grease Lubrication in Rolling Bearings," *Tribology Transactions*, **52**(5), pp 581–590.

(30) SKF Group. (2016), *SKF Rolling Bearings Catalogue*, SKF Group: Author.